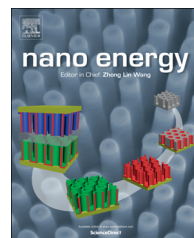




Available online at www.sciencedirect.com

ScienceDirect

journal homepage: www.elsevier.com/locate/nanoenergy



RAPID COMMUNICATION

Q2 Environmental effects on nanogenerators**Q1 Vu Nguyen, Ren Zhu, Rusan Yang****Department of Mechanical Engineering, University of Minnesota, Minneapolis, MN 55414, USA*

Received 2 October 2014; received in revised form 17 November 2014; accepted 25 November 2014

KEYWORDS

Nanogenerator;
Environmental effect;
Temperature;
Humidity;
Adsorption;
Pressure

Abstract

The desire for self-powered nanosystems and wearable devices has driven wide investigation of the sustainable energy source. Harvesting energy from the ambient environment with nanogenerators becomes a viable solution with the development of low-power electronics. Different devices can face dramatically different working conditions, which may seriously restrict the application of those nanogenerators. In this review article we describe the most recent progress in the study of the environmental effect on the nanogenerator. While a variety of nanogenerators have been developed using piezoelectric, triboelectric, pyroelectric and thermoelectric effects, the most studied piezoelectric nanogenerator and triboelectric nanogenerator will be discussed in more detail. This review emphasizes the important effect of the temperature, humidity, and water. The other effects, such as UV radiation or adsorption of gas or solid material, are also presented for certain nanogenerators. In the end we share our views of the future research directions and the remaining challenges in this field.

© 2014 Published by Elsevier Ltd.

Introduction

Renewable energy technologies have received dramatic interest with the increasing concerns of the climate change and the energy crisis. The renewable energy from solar and wind is contributing more and more in recent years at large scale. At much smaller scale, devices are normally powered by batteries and they are also in desperate needs for sustainable energy source that is of similar or smaller size. The development of

small size electronics with significantly reduced power consumption makes it possible to be powered with the energy harvested from their environment, and the small energy harvesters with nanomaterials or nanostructures are nowadays called nanogenerators. The development of the nanomaterials and nanotechnology leads to the first demonstration of the nanogenerator in 2006 with zinc oxide (ZnO) nanowires [1]. After that various nanogenerators [2] have been developed using piezoelectric [3-6], triboelectric [7], pyroelectric [8-10], and thermoelectric effects [11,12]. The nanogenerator is expected to complement or even replace batteries and facilitate the development of the self-powered nanosystems [13] and it also finds viable application for biosensors [14], chemical

*Corresponding author. Tel: +1 612 626 4318.

E-mail address: yangr@umn.edu (R. Yang).

1 sensors [15-17], photodetector [18-20], civil infrastructure/
 2 environment monitoring [21], and even portable/wearable
 3 personal electronics [22,23].

4 The wide application potential also brings new challenges to
 5 the nanogenerators. Different devices may work at dramatically
 6 different working environment, and the working condition
 7 of a device might change over its life span. For instance, the
 8 implantable medical device needs to live with fluid, the
 9 structural health monitoring system needs to survive the
 10 temperature change through the year, and the portable
 11 personal electronics may be placed in different environments
 12 at different time. Consequently, it is important to know clearly
 13 the environment effect on the nanogenerator and what is the
 14 limit of the nanogenerator to work properly.

15 The nanogenerator's responses to different environmental
 16 effects are determined by their working mechanisms and
 17 construction materials. For instance, the nanogenerator with
 18 solar cell [24-27] relies on the access to the light, while the
 19 nanogenerator based on pyroelectric effect and thermoelectric
 20 effect depends on the temperature change over time or
 21 spatial temperature gradient. Mechanical energy is the most
 22 ubiquitous and accessible energy source in the surroundings
 23 from the human activity, machine or infrastructure vibration,
 24 wind, or liquid flow. Most nanogenerators to date are designed
 25 to harvest the mechanical energy using piezoelectric effect or
 26 triboelectric effect. A few review articles [2,7,13,28-36] have
 27 provided great introduction to various piezoelectric nanogen-
 28 erators and triboelectric nanogenerators and thorough discus-
 29 sion of their working mechanisms. This article will focus on
 30 current progress in the study of the environmental effect on
 31 those nanogenerators.

32 The piezoelectric nanogenerator and the triboelectric
 33 nanogenerator will be discussed separately. Although some
 34 nanogenerators can work over a large temperature range,
 35 nanogenerators can be affected by temperature significantly.
 36 The exposure to different humidity or gases is very common in
 37 many applications, and their effects are reviewed for both
 38 types of nanogenerators. In addition, we paid special atten-
 39 tion to the effect of radiation on the piezoelectric nanogen-
 40 erator and the effect of the water and pressure on the
 41 triboelectric nanogenerators. The study of the environmental
 42 effect reveals the feasible working condition for the nano-
 43 generator and those effects can also inspire sensing applica-
 44 tions. Future research directions and the remaining challenges
 45 to understand and take advantage of the environmental effect
 46 on nanogenerators will be discussed.

47 Environmental effect on piezoelectric 48 nanogenerators

49 Piezoelectric materials have non-centrosymmetric crystal struc-
 50 tures and their centers of positive charge and negative charge
 51 are separated under mechanical stress. A piezoelectric nano-
 52 generator is typically built from one-dimensional piezoelectric
 53 nanostructures, such as wurtzite ZnO [37], CdS [38], ZnS [39],
 54 and GaN [40], β phase PVDF polymer [41], perovskite PZT [42],
 55 BaTiO₃ [43], NaNbO₃ [44], trigonal Te [45], etc. When those
 56 nanostructures are deformed by mechanical stimuli, such as
 57 body motion, acoustic wave, wind, and machine vibration, the
 58 charge separation builds up a piezoelectric potential which
 59 induces a current flow in external circuits and drives devices.

60 Compared with bulk materials, the nanostructures have much
 61 smaller dimensions and can be integrated into a nanosystems
 62 to power nanodevices. Some single crystalline nanostructures
 63 also have much better mechanical property than their bulk
 64 counterparts and therefore allow higher power density.
 65 Researchers show that high-quality ZnO nanowire has a high
 66 tensile fracture strain of $5 \pm 1.5\%$ and can sustain a 1.8% cyclic
 67 bending strain without fatigue [46-48].

68 Environmental factors can change the property of piezo-
 69 electric nanostructures and thus the performance of the
 70 nanogenerator. Piezoelectric property, which is represented
 71 by piezoelectric coefficients, determines how mechanical
 72 energy is converted into electric energy. The piezoelectric
 73 property can be damaged under extreme conditions such as
 74 high temperatures and ionizing radiation. For certain piezo-
 75 electric materials with semiconductivity, such as ZnO and
 76 GaN, the energy generation not only depends on the piezo-
 77 electric property but also their semiconductivity. Free
 78 charge carriers in the material partially screen the piezo-
 79 electric potential and lower the power output. Numerical
 80 analysis shows that a donor concentration of $N_D = 1 \times 10^{17}$
 81 cm⁻³ reduces the piezoelectric potential on the stretched
 82 side of a bent ZnO nanowire by 80% compared to an
 83 insulating nanowire without any charge carrier [49]. Environ-
 84 mental factors can significantly influence the free carrier
 85 concentration in the material through chemical and/or
 86 physical process, and change the output of nanogenerator.

87 In this section, we introduce some research work on how
 88 environmental factors affect the energy conversion through
 89 their influence on the piezoelectric property and/or the
 90 electric property of piezoelectric nanostructures. Common
 91 influential factors include temperature, humidity, adsorp-
 92 tion of oxygen, adsorption of other substances, and radia-
 93 tion. On one hand, understanding of the environmental
 94 impact facilitates the design of nanogenerator packaging to
 95 avoid adverse effects. On the other hand, nanogenerators
 96 with high sensitivity to environmental factors can serve as
 97 active sensors to monitor the humidity, UV light, gas, etc.

98 Temperature effect

99 A piezoelectric material will lose its permanent electric
 100 dipoles above a transition temperature, usually its Curie point
 101 or melting point, whichever is lower. The Curie temperature of
 102 BaTiO₃ is 130 °C and becomes lower with impurities [50]. The
 103 Curie temperature of β -PVDF is estimated to be higher than its
 104 melting point which is generally 175-185 °C [51]. However,
 105 long-term annealing can reduce the piezoelectric coefficient
 106 of PVDF at a temperature well below its melting point.
 107 Researchers annealed PVDF samples at elevated temperatures
 108 for 24 h and then measured their d_{33} value (piezoelectric
 109 charge constant) [52]. Figure 1a reveals that the d_{33} coeffi-
 110 cient monotonically decreases with temperature when the
 111 annealing temperature exceeds 80 °C. PVDF only retained 32%
 112 of its original d_{33} value after the 24-hour annealing at 140 °C.
 113 The thermal depolarization is probably due to the relaxation
 114 and reorientation of polymer chains. The inorganic piezo-
 115 electric ceramics, such as PZT, also lose their piezoelectric
 116 property when annealed below the Curie point [53]. Since a
 117 nanogenerator is expected to stay in the environment for an
 118 extended period of time, the long-term thermal stability of its

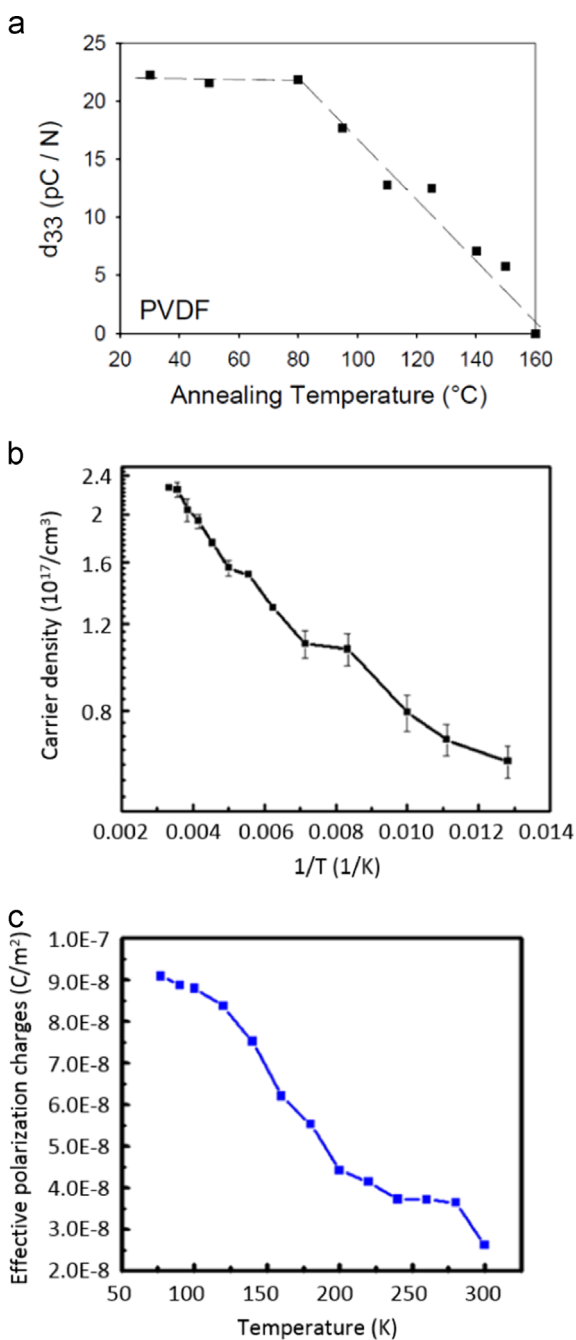


Figure 1 Effect of temperature on piezoelectric nanogenerators. (a) Change in the d_{33} coefficient of PVDF with the annealing temperature. Each data point was obtained after 24 h of annealing in air. Reprinted with permission from [52] (© 2005, Wiley). (b) Carrier density change in a ZnO nanowire as a function of inverse temperature. (c) Temperature dependence of effective piezoelectric charges at the ZnO nanowire's end surface. Reprinted with permission from [56] (© 2008, American Chemical Society).

piezoelectric property must be considered to determine the operation temperature. The service temperature of a piezoelectric material may not exceed half of its Curie point (as measured in °C) as a rule of thumb [54].

For nanogenerators based on wurtzite ZnO, the transition temperature is its melting point of 1975 °C. ZnO may sublime, but not below 1000 °C at ambient pressure. However, the semiconductivity of ZnO is more sensitive to the temperature. ZnO crystals almost always have unintentional n-type conductivity, with intrinsic defects and impurities as shallow donors [55]. As the temperature decreases, fewer dopant sites are thermally activated, lowering the carrier concentration.

Hu et al. put ZnO nanowire-based nanogenerator on a cryostat and investigated the temperature effect on the output [56]. Two silver electrodes were applied to form the Schottky contacts with the nanowire. The current-voltage ($I-V$) curves of the nanowire at different temperatures and strains were measured. Fitting of the $I-V$ curves based on a metal-semiconductor-metal transport model reveals semiconductor parameters including carrier concentration and the effective Schottky barrier height ϕ [57]. Piezoelectric charge partially determines ϕ [58], and thus can be calculated. In a typical test, when the temperature decreased from 300 K to 77 K, the carrier density in a nanowire decreased from $2.2 \times 10^{17} \text{ cm}^{-3}$ to $6 \times 10^{16} \text{ cm}^{-3}$ due to the donor freeze-out, Figure 1b. More importantly, when the mechanical input was kept the same, piezoelectric charge density on the end surface of the nanowire increased from about $2.6 \times 10^{-8} \text{ cm}^{-2}$ at 300 K to $9 \times 10^{-8} \text{ cm}^{-2}$ at 77 K, Figure 1c [56]. Enhancement of the piezoelectric output comes from the suppressed screening effect at lower temperatures. Q4

As the temperature increases from 300 K, it is expected that a larger percent of donors become activated. Nevertheless, the carrier density does not necessarily increase, because the heating may invoke other process that can change the carrier density. For example, hydrogen-related defects such as O-H centers are believed to be important shallow donors in ZnO. Shi et al. annealed a ZnO specimen at 150 °C in an inert gas, and then found that O-H infrared signature lines disappeared and carrier density dropped by 80% [59]. Therefore the heating effect depends largely on the property of ZnO source material.

Oxygen and humidity effect

Ambient air always contains oxygen and variant amount of water vapor, which could affect the piezoelectric materials and thus the performance of nanogenerators. ZnO is the most studied material for the piezoelectric nanogenerator and we will use it to elaborate the oxygen and humidity effect. At room temperature, oxygen molecules are adsorbed at surface defect sites of ZnO and gain electrons to form ions through the process: $\text{O}_2 + e^- \rightarrow \text{O}_2^-$ [60]. This process reduces the population of free electrons in ZnO and its effect becomes significant as the surface-to-volume ratio increases when the nanowire radius decreases [61]. Xue et al. tested an unsealed ZnO nanogenerator in gases with different oxygen concentrations [62]. Under the same mechanical actuation, the voltage output increased from 0.45 V in dry air to 0.7 V in pure oxygen, simply because more adsorbed oxygen mitigated the screening effect. Similarly, treatment with oxygen plasma is an effective way to improve the output of ZnO nanogenerators [63,64].

While oxygen is beneficial to the ZnO nanogenerator, moisture is not. Zhu et al. tested a ZnO nanogenerator with the relative humidity (RH) varied between 5% and 85% [65]. As shown in Figure 2a, the voltage output decreased as the humidity increased, and dropped by ~33% from 5% RH to 85% RH [65]. The reduction in the piezoelectric potential is due to the increased conductance of ZnO nanowire at a higher humidity. Several mechanisms may be involved in the humidity sensitivity of ZnO. The first mechanism is electronic-type conduction. As the humidity increases, there are more physically adsorbed water molecules on the ZnO surface. Dipoles of the water molecules will line up and neutralize the surface electric field, rendering the electron on O_2^- in an unfavorable energy state. Some oxygen ions release electrons back into the conduction band of ZnO and increase the surface conductance [66]. The second mechanism is ionic-type conduction. Dissociation of water molecules produces H_3O^+ groups. When water molecules do not cover the whole surface of ZnO, the conduction happens through hopping of H_3O^+ between adjacent hydroxyl groups on the surface. After the physisorbed water layer becomes continuous, protons can hop between adjacent water molecules just like in liquid water (Grotthuss chain reaction) [67].

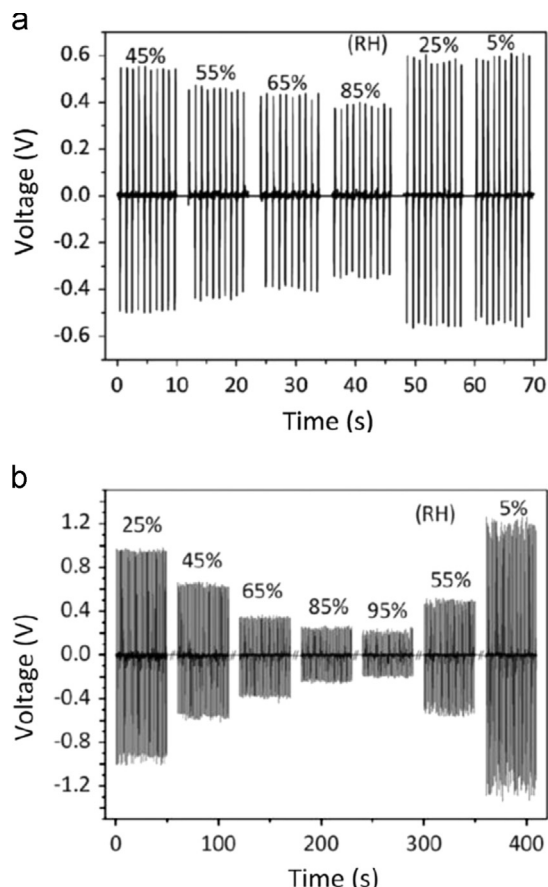


Figure 2 Effect of humidity on piezoelectric nanogenerators. (a) The piezoelectric output voltage of bare ZnO nanowires at different humidities under the same deformation. (b) The piezoelectric output voltage of CeO₂-coated ZnO nanowires at different humidities under the same deformation. Reprinted with permission from [65] (© 2014, Elsevier).

The humidity effect could be more aggressive when the ZnO surface is modified. In the same study from Zhu et al., CeO₂ and SnO₂ nanoparticles were applied onto the surface of ZnO nanowires [65]. The nanoparticles increase the surface area for water adsorption and facilitate the dissociation of water molecules, making the nanogenerator more vulnerable to the humidity. Figure 2b is the voltage output of a CeO₂-modified device at different humidities. The voltage dropped by ~82% from 5% RH to 85% RH [65]. A comparison of Fig. 2a and b clearly shows the effect of CeO₂. Although the surface modification is unfavorable in terms of power generation, it increases the sensitivity if the device is regarded as a self-powered humidity sensor.

Aforementioned studies focus on the ZnO nanogenerator, but the principle applies to other piezoelectric nanogenerators. For insulating piezoelectric materials, adsorption of water vapor leads to ionic-type conduction on the surface that increases leak current of the generator. Dielectric property, which also affects the energy generation, may change with the adsorbed water as well. Many nanogenerators are metal oxide with large surface area and tend to adsorb water vapor. For instance, from 20% RH to 80% RH, nanocrystalline BaTiO₃ experienced a two-order-of-magnitude decrease in resistance and significant increase in dielectric constant at low frequencies [68,69]. In another case, porous PZT showed a large resistivity change from $10^{14} \Omega \text{ cm}$ to $10^7 \Omega \text{ cm}$ for a relative humidity from 5% to 85% [70].

Insulating perovskite ferroelectrics may possess semiconductivity with doping. BaTiO₃ shows n-type conductivity with oxygen vacancies or metal ions as donors [71]. In addition to the ionic-type conduction, adsorbed water may donate electrons to the n-type BaTiO₃ and promote the electronic-type conduction, especially at higher temperatures (~400 °C) [72]. On the other hand, oxygen as an electron acceptor has been reported to reduce the conductivity of Nb-doped BaTiO₃ at elevated temperatures (>1000 K) [73]. Although the effect of water or oxygen on the semiconductivity of BaTiO₃ is insignificant below its Curie point, the semiconductivity is always unfavorable for energy generation and impurities should be avoided during the material synthesis.

Adsorption effect

Substances other than oxygen and water can be present in the environment and become adsorbed onto the surface of nanogenerators. Since nanostructure has a large surface-to-volume ratio, surface effect from the adsorption could change the device behavior significantly. Here we discuss the adsorptions that affect the energy generation via resistance change. Most changes are reversible upon desorption. Some chemicals that attack the bulk part of the material and irreversibly change its composition (such as etching) will not be covered.

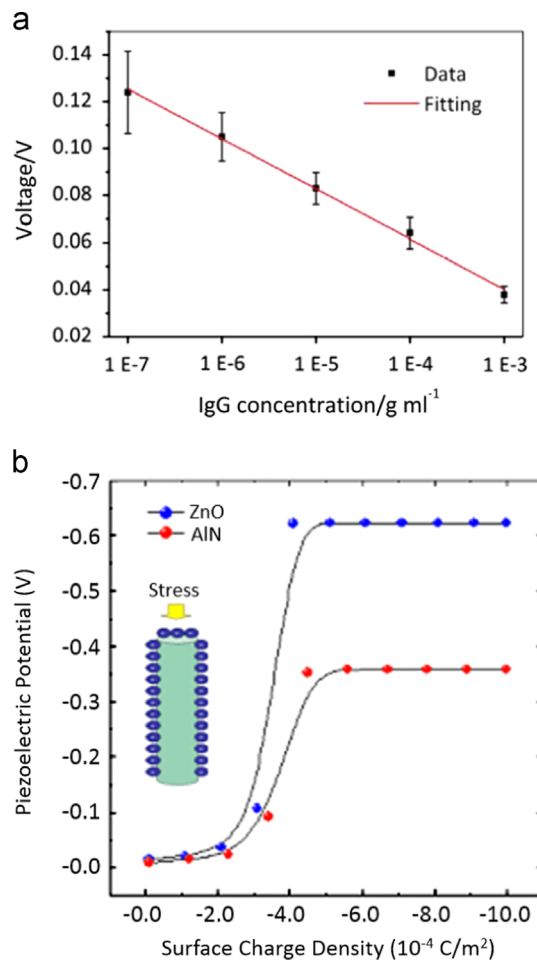
Current research in the literature is focused on how the adsorbates affect the output of ZnO nanogenerator. As mentioned earlier, oxygen as an oxidizing gas gains electrons from the n-type ZnO and lowers its carrier density. Similarly, some reducing gases could inject electrons into ZnO and increase its carrier concentration, aggravating the screening effect. Xue et al. exposed ZnO nanogenerator to H₂S, which is a pollutant with strong reducing characteristics [62]. H₂S reacts with the

1 chemisorbed oxygen on the ZnO surface, causing the electrons
 2 in the oxygen ions to flow back into ZnO [$2\text{H}_2\text{S} + 3\text{O}_2^- \rightarrow 2\text{SO}_2 + 2\text{H}_2\text{O} + 3\text{e}^-$]. An H₂S level as low as 100 ppm lowered
 3 the device output from 0.45 V to 0.398 V, and 1000 ppm further
 4 reduced it to 0.198 V [62]. Ethanol is another reducing agent in
 5 the environment. Catalytic dissociation of ethanol produces
 6 hydrogen, which reacts with oxygen ions on the ZnO surface
 7 and increases the electron concentration [$4\text{H} + \text{O}_2^- \rightarrow 2\text{H}_2\text{O} + \text{e}^-$]. Zhao et al. decorated ZnO nanowires with plati-
 8 num nanoparticles as catalyst, and studied the effect of
 9 ethanol vapor on the piezoelectric performance [74]. Exposure
 10 to 1500 ppm ethanol at room temperature reduced the output
 11 by 38%. The generator was also tested with methanol, acetone
 12 and formaldehyde, and experienced similar degradation in its
 13 output [74]. To avoid the negative effect from reducing gases,
 14 the nanowires need to be properly sealed, for example in an
 15 epoxy [62].

16 Adsorption of external charges also affects the semicon-
 ductivity of ZnO nanogenerators. The adsorbed charges inter-
 act electrostatically with the internal free carriers and can be
 17 regarded as a floating gate. For n-type ZnO, positive charges
 18 are like a positive gate that attracts electrons and increases
 19 conductance, while negative charges deplete the internal
 20 electrons and decrease conductance [75]. Immunoglobulin G
 21 (IgG) is a biomaterial with positively-charged amino groups.
 22 Zhou et al. immersed a ZnO nanogenerator in IgG solutions
 23 for 1 h, followed by washing and drying [76]. After the surface of
 24 ZnO nanowires adsorbed IgG molecules, the positive charge
 25 from IgG increased the carrier density in ZnO and inhibited
 26 the power generation. Based on the measurement data in
 27 **Figure 3a**, soaking in more concentrated IgG solution caused a
 28 greater reduction in the voltage output [76]. On the same
 29 principle, negative charge adsorbed on n-type ZnO could
 30 enhance its power generation. Kim et al. theoretically inves-
 31 tigated the effect of negative charge on ZnO and AlN
 32 nanogenerators [77]. Both materials are assumed to have a
 33 typical donor concentration of 10^{17} cm^{-3} . As the surface
 34 adsorbs negative charge, the piezoelectric potential of nano-
 35 wires increases by more than one order of magnitude and then
 36 saturates, **Figure 3b**. The saturation corresponds to the
 37 complete depletion of free electrons in the nanowires [77].

38 Some adsorbates that are p-type semiconductors or high
 39 work function metals could form p-n junctions or the Schottky
 40 barriers with the n-type ZnO. Such interfaces induce a charge
 41 depletion region on ZnO surface and decrease the carrier
 42 density. Consequently, the screening effect is reduced and
 43 power output may be recovered. Lee et al. reported 18-fold
 44 enhancement in the voltage output of a ZnO nanogenerator
 45 after it was coated with a p-doped conjugated polymer [78].

46 With ZnO as an example, adsorbates decrease the resis-
 47 tance of n-type materials by injecting electrons (reduction)
 48 or inducing electron accumulation near the surface, and
 49 increase the resistance by extract electrons (oxidation) or
 50 creating an electron depletion region. For p-type semicon-
 51 ductors, reducing agents or hole depletion may raise the
 52 resistance, while oxidizing agents or hole accumulation may
 53 lower the resistance [66]. This rule can be generalized to
 54 non-wurtzite piezoelectric materials with semiconductivity.
 55 For instance, Jain et al. demonstrated that pure BaTiO₃ with
 56 oxygen vacancy or Cr-doped BaTiO₃ had n-type conductivity
 57 and reducing gases such as H₂S and NH₃ further increased
 58 the conductivity by injecting electrons; this effect became



59 **Figure 3** Effect of external charge adsorption on piezoelectric
 60 nanogenerators. (a) The piezoelectric output of a ZnO nano-
 61 generator after being immersed in different concentrations of
 62 IgG solution. Reprinted with permission from [76] (© 2014,
 63 Elsevier). (b) Calculated piezoelectric potential of ZnO and AlN
 64 nanowires with different densities of adsorbed negative charge.
 65 Reprinted with permission from [77] (© 2012, authors).

66 more significant as temperature rose from room tempera-
 67 ture and peaked around 350 °C [79]. Barium strontium
 68 titanate (BST) is another ferroelectric perovskite. Roy
 69 et al. showed that at elevated temperatures Ba_{0.5}Sr_{0.5}TiO₃
 70 was p-type and NH₃ reduced its conductivity [80], as
 71 opposed to the n-type BaTiO₃. Variation of the resistance
 72 due to adsorbates will change the leak current of the
 73 piezoelectric materials and affect the power generation.

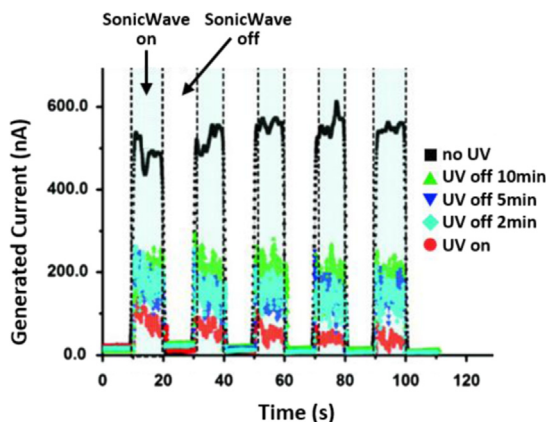
Radiation effect

74 In extreme environment like nuclear reactors and outer space,
 75 high-energy radiations such as gamma ray and neutrons can
 76 deteriorate piezoelectric materials. PVDF experiences changes
 77 in its mechanical property and crystallinity under irradiation,
 78 due to chain scission and crosslinking reactions [81,82]. Piezo-
 79 electric ceramics could be depoled by thermal spike (localized
 80 heating above the transition temperature), or amorphized
 81 by displacement spike (atoms permanently displaced from
 82 lattice sites). Wurtzite ZnO and AlN are promising piezoelectric

1 materials that can have application in harsh radiation environment, because of their high transition temperatures and
 3 resistance to amorphization [83].

5 Nanogenerators are usually considered to operate in our ambient environment, where high-energy radiation is rarely encountered. However, UV radiation from the sun or artificial sources could change the electronic property of semiconducting ZnO. The surface of ZnO nanowire has defect sites that adsorb oxygen molecules. The chemisorbed oxygen captures free electrons and forms a thin depletion layer, which causes upward band bending of ZnO near the surface. During illumination, photons with energy larger than the band gap (wavelength <367 nm) are absorbed and generate electron-hole pairs. Some holes migrate towards the surface under the band bending and discharge the negatively-charged oxygen ions, leading to the desorption of oxygen molecules [$O_2^- + h^+ \rightarrow O_2$]. The unpaired electrons increase the carrier density inside ZnO and partially screen the piezoelectric charge. After the UV light is off, re-adsorption of the oxygen on the ZnO surface gradually reduces the free electron density to its initial value [20,84,85]. Liu et al. used ultrasonic wave to excite a direct-current ZnO nanogenerator and studied the UV effect [86]. As shown in Figure 4, in the dark environment, the nanogenerator output a current of ~500 nA. As soon as the UV light was on, the current output decreased to 30-80 nA. After the UV light was off for 2, 5, and 10 min, the current increased to ~180, 190, and 205 nA, respectively. The slow recovery of the current output is due to the re-adsorption process of the oxygen.

29 Since the hole trapping process is associated with the desorption and adsorption of oxygen on the surface, one would anticipate that the photoresponse depends on the 31 surface condition and ambient gas. If the nanowire is in 33 vacuum instead of atmosphere, the re-adsorption of oxygen 35 will be more difficult [85,87]. It results in a much slower decay 37 of the photo-induced carriers after the UV is off, and the 39 adverse effect of the UV light on the piezoelectric output will 41 last longer. Another example is annealing. Pham et al. demonstrated 43 that annealing makes ZnO nanogenerator less sensitive to the 45 UV irradiation [20]. In their experiment, as-synthesized ZnO 47 nanowires experienced an 80% drop in their voltage 49



57 **Figure 4** Current generated by a ZnO nanogenerator when the
 59 ultrasonic wave was turned on and off under different illumina-
 61 tion conditions of UV light. At first the measurement was in a
 dark environment, then the UV light was turned on, and finally
 the UV light was turned off. Reprinted with permission from
 [86] (© 2008, American Chemical Society).

63 output under the UV light. After annealing at 350 °C in air
 65 for 30 min, the output only reduced by 17% under the same UV
 67 light [20]. Annealing eliminates many defect sites on the ZnO
 69 surface, which reduces the number of adsorbed oxygen ions
 71 and also alleviates the band bending. As a result, fewer
 photogenerated holes are trapped and direct electron-hole
 recombination becomes dominant [84], so the impact of UV on
 the piezoelectric output is weakened.

Environmental effect on triboelectric nanogenerators (TENGs)

73 TENG are based on the two fundamental processes: contact
 75 electrification and electrostatic induction. Upon contact
 77 between the two working surfaces of the TENG, at least one
 79 of which is dielectric material, the surface with higher
 81 negative, or positive, charge affinity will attract negative,
 83 or positive, charges from the other surface. Once the
 85 charges are transferred, the charges at the dielectric sur-
 87 face induce opposite charges on the electrodes. As the two
 89 working surfaces move relatively to each other, the induced
 91 charges move across the external circuit to provide power
 93 to external loads. The effect of the environment on TENG
 95 will be discussed through their influence on contact elec-
 97 trification and electrostatic induction.

Temperature effect

99 As the applications for TENGs expand, operations under extreme
 101 conditions may be required. Among the environmental para-
 103 meters, temperature is the one that can readily affect the TENG
 105 due to heat transfer to or from the device. It is imperative to
 107 verify the applicability of TENG in a wide range of tempera-
 109 tures. Since TENG's working principles are mainly based on two
 111 processes: contact electrification and electrostatic induction,
 113 the temperature-dependence of these two processes greatly
 115 influences the overall performance of the TENG.

117 Temperature has a significant effect on the contact elec-
 119 trification, which is the charge transfer between two contacted
 121 surfaces, of the TENG [88]. The temperature-dependence of
 123 contact electrification can be explained by the thermal
 fluctuation that is a new driving force for charge transfer,
 and the change of the mechanical property of the contacted
 material that affect the contact area. In order to investigate
 this dependence, a triboelectric pair, polytetrafluoroethylene
 (PTFE) and aluminum, was in [88] selected due to their highly
 opposite charge affinity. The tested temperature range was
 from 77 K to 500 K, which covers almost the entire working
 range of PTFE as specified by the manufacturer. Figure 5 shows
 the experimental setup and two plots, open-circuit voltage and
 short-circuit current versus temperature. The experiments
 were carried out in two setups: high temperature and low
 temperature, and the results were combined and normalized
 with respect to the result at room temperature. As tempera-
 ture increases from 77 K to 500 K, both the open-circuit
 voltage and short-circuit current first increase to a maximum
 value, at around 260 K, and then decrease monotonically.

121 The nanogenerator's response to the temperature can be
 123 explained by the competing effects between the change in
 thermal fluctuation and the change in mechanical properties
 [88]. As the temperature increases, the thermal fluctuation

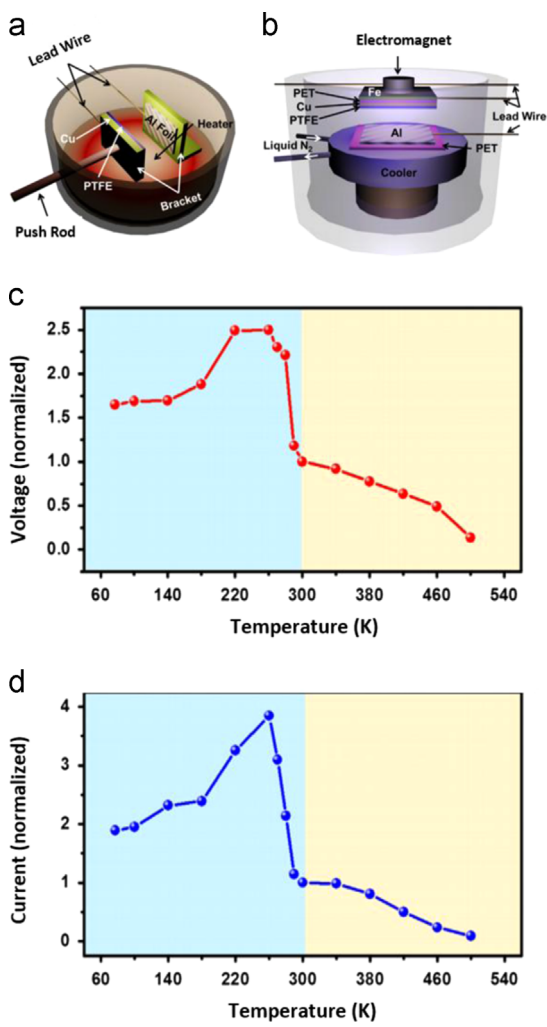


Figure 5 Test of temperature effect on aluminum-PTFE TENG. (a) High-temperature setup. (b) Low-temperature setup. (c) Open-circuit voltage normalized to value at room temperature. (d) Short-circuit current normalized to value at room temperature. Reprinted with permission from [88] (© 2014, Elsevier).

caused more charge transfer in the backward direction, i.e. the transfer of negative charges from PTFE surface to aluminum surface, as opposite to the desired forward direction from aluminum to PTFE surface. The increase of backward charge transfer lowered the overall balanced charges on the two contacted surfaces, which lowered net negative charges on PTFE surface and degrades the output. On the other hand, as temperature increased from 77 K to 500 K, a polymer surface like PTFE transformed from a glassier surface to a softer one. The softer surface facilitated more deformation at nanoscale. The increased contacted surface area benefited the charge transfer and enhanced the output. The effects of both the thermal fluctuation and the softness of the PTFE surface contributed to the nanogenerator performance simultaneously. At lower temperature, from 77 K to 260 K, the change in softness of the PTFE surface had dominant effect, so increasing open-circuit voltage and short-circuit current were observed. The opposite was true for temperature above 260 K. In both extreme ends of the temperature range, the TENG was able to light up several LEDs connected in series,

with the lowest efficiency at 500 K and the highest efficiency at 260 K. The results from this study suggest that employing TENG in a low temperature environment can be a good approach to improve its efficiency, as long as it does not compromise the contact area due to the change in mechanical properties. For high temperature applications, selecting materials that have highly opposite charge affinity can potentially lower the effect of thermal fluctuation.

In addition, temperature can have a significant effect on the electrostatic induction process, especially for materials that have their dielectric constant sensitive to temperature. One such material is water that has been used as a working electrode of TENG. Unlike PTFE in the previous study, which has its dielectric constant reduce only about 10% over 23–314 °C range [89], water has its dielectric constant reduce nearly 30% over 70 °C [90]. When water was served as an electrode, increasing temperature significantly decreased the short-circuit current density [91], which can be attributed to the reduction of dielectric constant of water.

It is important to note that TENG contact electrification and electrostatic induction happen simultaneously under the temperature's influence and that the temperature change the mechanical and electric properties of the different contact materials to a different extent. The temperature effect on the overall performance of the TENG is a collective result of more than one process. Understanding how temperature affects each process can help the material selection and rational design of an optimum TENG for a particular application.

Humidity/water effect

The ubiquitous water content in the environment, whether in vapor or liquid phase, may penetrate through the TENG's package into the gap between two contacted surfaces. The contact electrification process in TENG can be influenced by this water penetration because water can fill the gap or adsorb as a thin layer onto each surface during the operation of TENG. This influence generally depends on the wettability of the working surfaces and the amount of water present, as demonstrated by a study in [17].

Figure 6 shows the experimental data from [17] for two TENGs, one using hydrophilic polyamide 6, 6 (PA) and the other using hydrophobic PTFE. The second working surface is aluminum in both TENGs. The results clearly shows that the water droplet on hydrophilic PA surface almost eliminates all the charges from contact electrification, indicated by negligible open-circuit voltage of the TENG. On the other hand, the water droplet has almost no effect on the performance of the TENG made from PTFE. The results are similar for TENGs made from hydrophilic Kapton film and hydrophobic polydimethylsiloxane (PDMS). This observation can be explained by the fact that hydrophilic surfaces tend to retain water, which spreads over a larger area. This liquid water layer shields the surfaces and prevents the effective charge transfer between the two contacted surfaces. Thus the TENG's output is degraded. For hydrophobic surfaces, the water droplet can be easily pushed away from the contacted area as the TENG operates. Even if it is retained on the working surfaces, the covered area is small. Thus its effect on hydrophobic surface is negligible.

The same trend was also observed when water penetrates into TENG in the form of vapor, which is quantified by relative

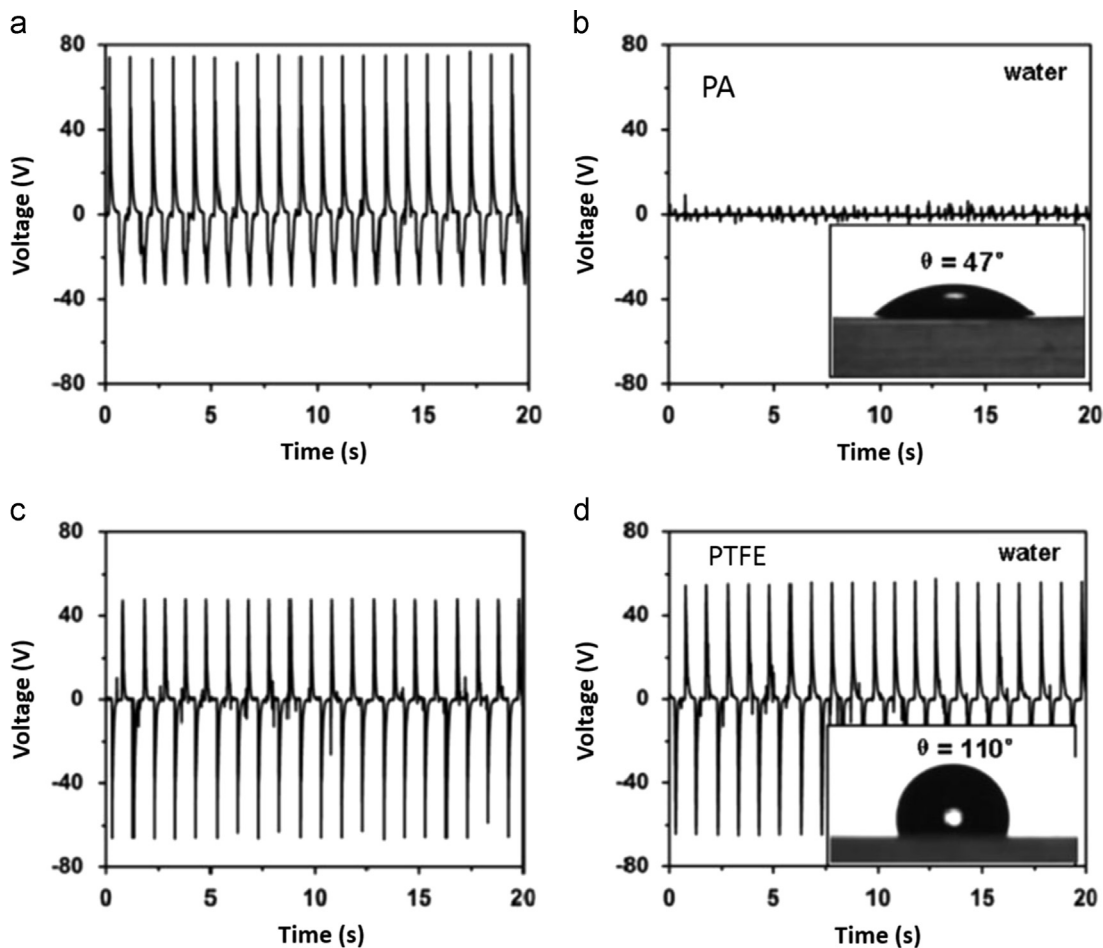


Figure 6 Effect of a water droplet on the hydrophilic and hydrophobic surfaces of the TENG. Open-circuit voltage of the aluminum-PA TENG (a) before and (b) after the introduction of the droplet. Open-circuit voltage of the aluminum-PTFE TENG (c) before and (d) after the introduction of the droplet. Reprinted with permission from [17] (© 2013, Elsevier).

humidity (RH). As shown in Figure 7, for hydrophilic PA surface, the open-circuit voltage of TENG decreases exponentially with RH, while for hydrophobic PTFE surface the effect of RH is not as significant. To explain this observation, it is important to note that even in the absence of water droplet, there is often a nanoscale layer of water adsorbed onto the polymer surface and the effective thickness of this layer is suggested to play a key role in the charge transfer between two contacted surfaces [92]. The experimental data suggests that the thickness of this nanoscale adsorbed water layer on hydrophilic surfaces is more sensitive to RH than that on hydrophobic surfaces.

The above results indicates that depending on the materials used, or specifically the hydrophilicity of the material, TENG can be either very sensitive or very insensitive to the water content of the environment. Consequently, an appropriate material selection and/or surface modification can result in a TENG that can effectively serve as either a stable energy harvester or a sensitive liquid/gaseous water detector.

It is also worth noting that the effect of the hydrophilicity of the surface found with water as the liquid can also be applied to other liquid as well. For example, PTFE is hydrophobic to pure water but hydrophilic to ethanol. Thus PTFE-based TENG still shows significant response to the penetration of ethanol [17].

In the above cases, the introduction of water into the TENG often has a negative effect on the TENG's output. However, in other designs of TENG, water can be beneficial or even required. Water was demonstrated to serve as a working electrode for a TENG [91,93], or provide additional kinetic energy as in water wave [93]. The configurations of TENG with water as a working electrode were discussed in detail in [91] and [93]. Those studies demonstrated that water can work in both contact/separation mode [91] or sliding mode [93]. Figure 8 shows the schematic of the TENGs employing water in contact/separation mode and in sliding mode, as well as the obtained open-circuit voltage. In both cases water was charged positively when in contact with polymers such as Fluorinated Ethylene Propylene (FEP) or PDMS. When TENG worked in sliding mode, a moving water wave covered the polymer surface with different amount, causing the induced charges moving back and forth among the underlying metal electrodes. When TENG worked in contact/separation mode, varying distance between the polymer and the water surface caused the induced charge to move through the external circuit. In both cases where water served as a working electrode, the TENG could light up tens of LEDs connected in series. These studies proved that directly using the water as a working electrode can be

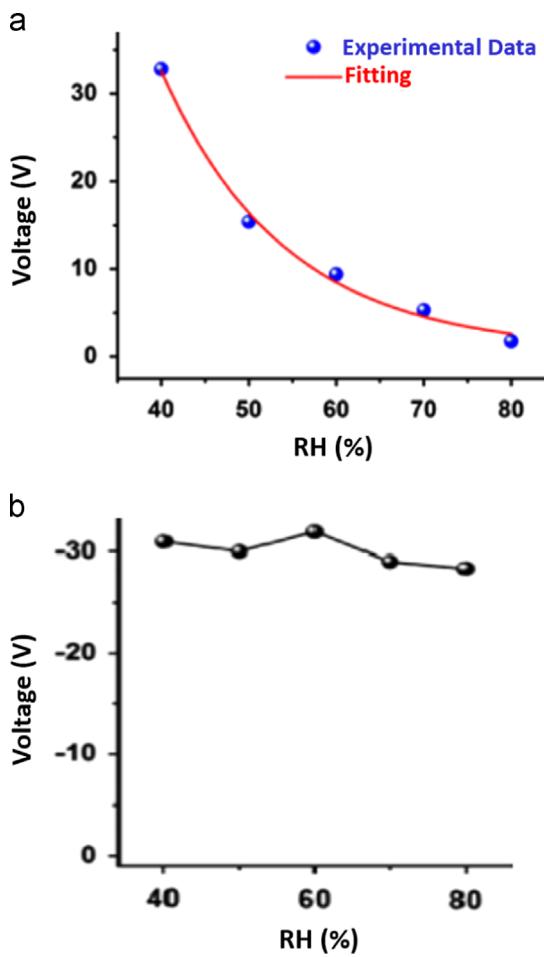


Figure 7 Dependence of the open-circuit voltage of TENG on RH. (a) an exponential decrease of open-circuit voltage with increasing RH for hydrophilic PA surface. (b) a slight variation of open-circuit voltage with RH for hydrophobic PTFE surface. Reprinted with permission from [17] (© 2013, Elsevier).

an approach to obtain high-performance TENG working in an aqua environment.

Adsorption effect

In some applications TENG may need to operate in the presence of various chemicals other than water, such as sea water energy harvesting, which exposes the TENGs to various ions. The desired response to these chemicals may be different. For instance, the self-powered chemical detection requires, high selectivity is toward the chemical of interest. These chemicals can change the property of the exposed surfaces or even the entire bulk. Two fundamental processes in TENG, i.e. contact electrification and electrostatic induction, can be altered by the exposure of TENG to chemicals.

Effect of chemicals on contact electrification in TENG can be explained by either physical or chemical adsorption onto the material surfaces. Chemical adsorption involves formation of chemical bonding between the adsorbent and the adsorbate, while physical adsorption only involves weak interactions such as van der Waal's force and is more reversible. The study in [17] demonstrated the effect of

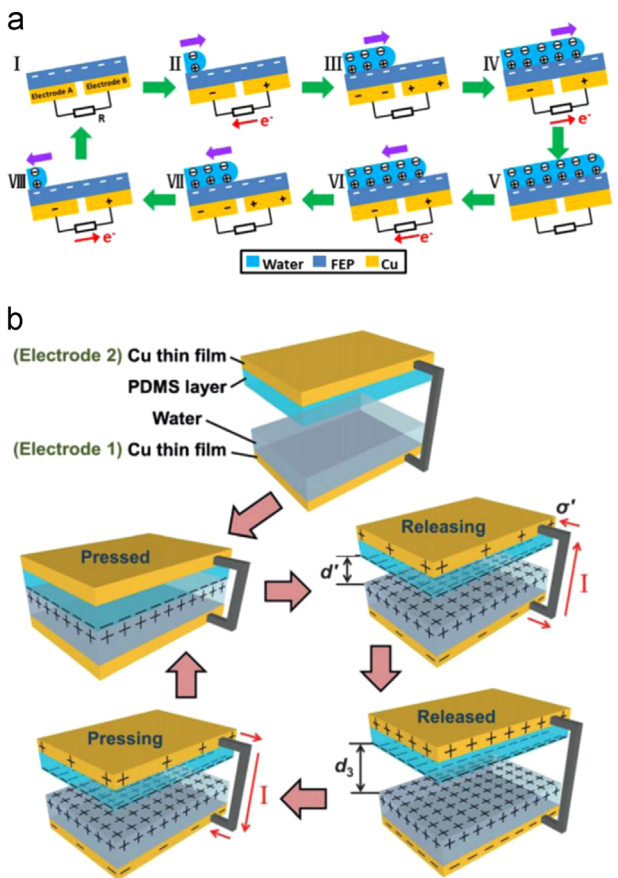


Figure 8 Schematic of TENGs which employ water as a working electrode. (a) sliding mode and (b) contact/separation mode water-based TENGs. Reprinted with permission from [91] (© 2013, Wiley) and from [93] (© 2014, Elsevier).

physical adsorption of the vaporized mixture of ethanol and water on TENG using PTFE as a working surface. Figure 9 shows the schematic of the device and the decreasing open-circuit voltage as the ethanol concentration in the vapor increases. It was shown from the same study that liquid mixture with higher ethanol concentration becomes more hydrophilic to the PTFE surface. This result suggests that vapor with higher ethanol concentration is more likely to adsorb onto the PTFE surface and further reduce the triboelectric charge. Due to the fast physical adsorption/desorption process, the recovery time is quite short (20 s) when the ethanol gas is turned off, which makes the TENG suitable for the ethanol sensing application.

While most chemical vapors can physically adsorb onto polymer surfaces, chemical adsorption has higher selectivity. Depending on the surface chemistry, only certain types of molecular species can chemically adsorb onto the surface and alter the contact electrification. For example, as shown in [94], gold nanoparticles (AuNPs), which are often used to enhance the output of TENG, can bind to 3-mercaptopropionic acid (3-MPA) due to Au-S bonding. 3-MPA, in turn, tends to bind mainly to Hg^{2+} ion among other metal ions due to its carboxylic acid group. Hence, if the AuNPs in AuNPs-based TENG are treated with 3-MPA, TENG is more sensitive to Hg^{2+} ion than other metal ions, as shown in Figure 10. This high selectivity is due to the selective bonding of the Hg^{2+} ion to

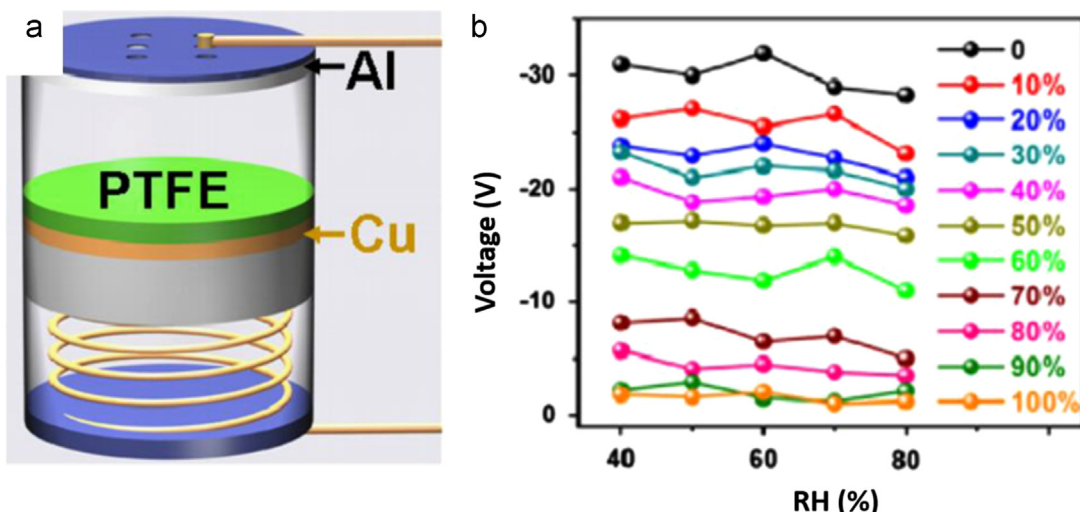


Figure 9 TENG ethanol vapor detector enabled by physical adsorption of the mixture of ethanol and water on PTFE surface. (a) Schematic of the TENG ethanol vapor detector and (b) its response to different concentrations of ethanol. Reprinted with permission from [17] (© 2013, Elsevier).

the treated AuNPs and the change of the triboelectric charge affinity as a result. The chemical adsorption of certain species from the environment may affect the output of the TENG more significantly than others. Tuning the chemical adsorption with surface modification can be a controllable approach to obtain a desired TENG for either a sensitive chemical sensor or an enhanced energy harvester.

In some cases, chemicals can penetrate into the bulk of the working material and change its electrical properties, such as dielectric constant or the number of free ions. When the TENG employs liquids such as water as a working electrode, this effect can be dominant. For example, the study in [91] demonstrated that ethanol content reduced the dielectric constant of water and had a similar detrimental effect on the output of as the increased temperature that was discussed previously. The dissolution of salt in the water increases significantly the number of free ions within the working material. These free ions can adhere to the surface of the opposite charge, decrease the charge induced to the external circuit, and lower the nanogenerator output [91]. Data shown in Figure 11 agree with this suggestion by showing that the increased ion content in water, as in tap water and 0.6 M NaCl solution compared to deionized water, has a detrimental effect on the output of TENG. This problem can be overcome by good sealing/packaging of TENG from ionic materials, as well as by frequent cleaning/maintenance of the solid electrode.

Atmospheric pressure effect

Atmospheric pressure has been shown to affect the contact electrification process of TENG [95,96]. It has been suggested that pressure takes effect through impacts on the equilibrium of the adsorbed charged species on the surface, and on the thickness of the adsorbed nanoscale water layer. The understanding of the pressure effect can serve as a guideline for designing TENG in a wide range of pressure.

The equilibrium of the adsorbed charges on the dielectric surface was proposed in [95]. In this model, the equilibrium is

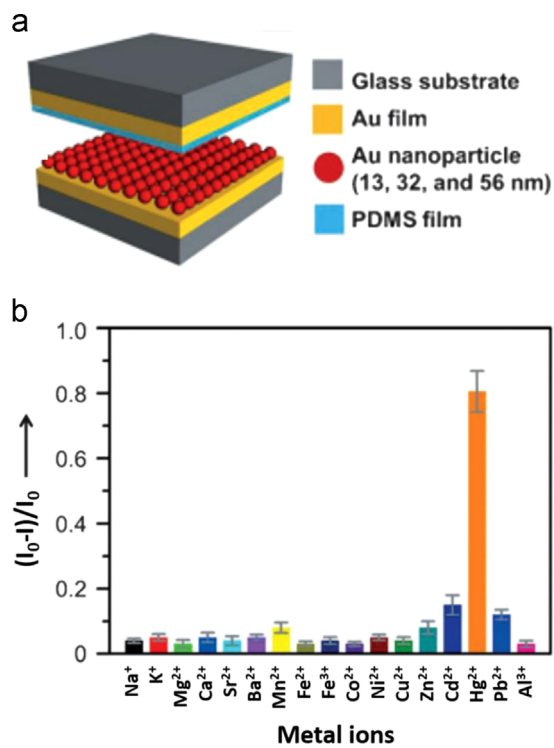


Figure 10 TENG Hg^{2+} ion detector enabled by chemical adsorption of Hg^{2+} to the chemically modified Au NPs-based TENG. (a) Schematic of the TENG Hg^{2+} ion detector and (b) its high selectivity toward Hg^{2+} among other metal ions. Reprinted with permission from [94] (© 2013, Wiley).

achieved when the chemical potential of the charge-containing adsorbed layer is equal to that of the ion-containing vapor at the surface. When the atmospheric pressure changes, the chemical potential of the vapor also changes. This change shifts the equilibrium and thus changes the charge density of the adsorbed layer. Experimental data were obtained in the study for a series of dielectric materials and they agree with the author's model. The data showed that as a charged

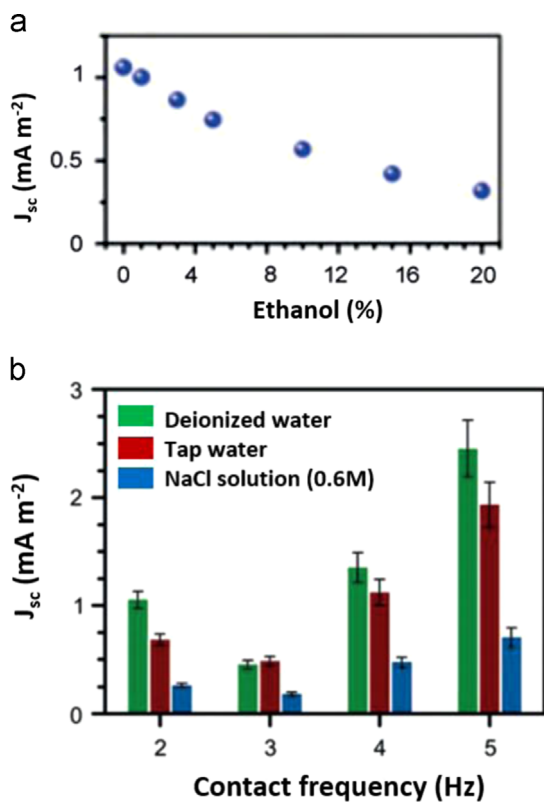


Figure 11 Dissolution/mixture of chemicals in water significantly affect the performance of water-based TENG. Short-circuit current density reduces with (b) increasing ethanol content, and (c) increasing ions content as in tap water and 0.6 M NaCl solution. Schematic of the tested TENG is provided in Figure 9b. Reprinted with permission from [91] (© 2013, Wiley).

dielectric surface was exposed to different pressure, decreasing pressure decreased the charge density on the dielectric surface. Although this effect may not be desirable for TENG, the study suggested that the effect of pressure on the retained charge can be reduced through choosing materials with proper adsorption energies.

The effect of pressure is not monotonic since the pressure also influences the thickness of the adsorbed water layer on many dielectrics. As the relative humidity (RH) changes with the atmospheric pressure, this adsorbed water can become thinner or thicker. The thickness is suggested to be key for charge distribution upon contact of the two working surfaces of TENG [92]. The section “Humidity/water effect” discussed that lower RH with thinner adsorbed layer increases transferred charges upon contact, so decreasing pressure can, unlike the case mentioned above, increase the output of the TENG as well. This competing effect was demonstrated in the study in [96]. Figure 12 shows the schematic of the tested TENG and its output as the pressure decreases with close-to-zero and non-zero RH. When RH is kept constant at approximately zero across the tested pressure range, output charge does decrease monotonically with pressure [95]. However, when the starting RH is higher, decreasing pressure first raises the output charge before lowering it. This peak can be attributed to competition between the lower equilibrium surface charge according to the model in [95] and the higher transferred charge due to thinner

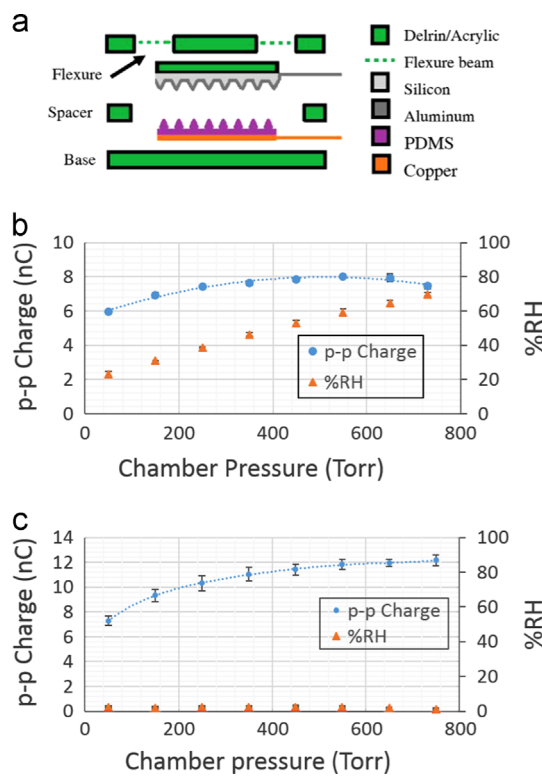


Figure 12 Effect of atmospheric pressure on the output of the TENG. (a) schematic of the tested TENG which employ aluminum-PDMS contact, and its output charge with (b) non-zero-RH atmosphere and (c) close-to-zero RH atmosphere. Reprinted with permission from [96] (© 2013, Elsevier).

adsorbed water layer. Therefore, a good knowledge in this behavior of the TENG can help in optimizing its performance for various pressure levels.

Conclusion

This article provides a comprehensive review of the state-of-the-art research on the environmental effect on nanogenerators. The nanogenerators with much improved performance are expected to provide sustainable self-sufficient micro/nanopower sources for future self-powered nanosystems in different working conditions. The service temperature of any device needs inevitably to be significantly lower than the melting temperature of the containing material, and it has been demonstrated that some nanogenerators are capable of working over a wide temperature. Curie temperature is another upper limit for all piezoelectric nanogenerators, and the temperature effect can be dramatic when the piezoelectric material also shows semiconducting property. Although the piezoelectric property is not very sensitive to the external environment, the influence on the charge carrier and conductivity in the piezoelectric materials can dominate the change of the nanogenerator output. Water extrusion or high humidity normally degrades the performance of both piezoelectric nanogenerators and triboelectric nanogenerators. Hydrophobic materials are preferred in a triboelectric nanogenerator when the water or humidity is a concern, while water can be used for the

1 energy conversion in an innovatively designed nanogenerator. In addition, the nanogenerator performance is also
 3 influenced by the gas exposure. The output can be either increased or decreased, depending on the different interaction
 5 of the nanogenerator with different gases. UV radiation clearly degrades the performance of some piezo-
 7 electric nanogenerators, while for triboelectric nanogen-
 9 erator detrimental effect of low pressure can be offset by humidity.

11 The study of the environmental effect is still at its early stage. The single-atomic-layer MoS₂ added to the expanding
 13 material family of nanogenerators [97]. Different materials can respond to the environment stimuli differently due to its
 15 properties and geometries. The theoretically computation and the experimental investigation are needed for a thorough and
 17 in-depth understanding of the energy conversion at different
 19 conditions, which will enable people rationally design a device working at various environments. The intertwined effect of
 21 different environmental factors will be a new challenge and needs to be resolved. A comprehensive understanding of the
 23 environmental effect will promote a wide and practical application of nanogenerators in self-powered systems in sensing,
 25 medical science, infrastructure/environmental monitoring, and personal electronics.

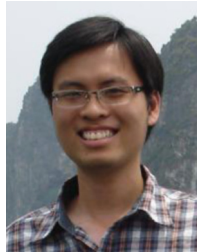
Acknowledgments

29 The authors are truly grateful for the financial support from
 Q6 the Department of Mechanical Engineering and the College
 31 of Science and Engineering of the University of Minnesota.
 Research is also supported by National Science Foundation
 33 under Grant no ECCS-1150147 and 3M Non-tenured Faculty
 35 Award. The device fabrication was performed in the Minnesota Nano Center, a part of NSF-funded National Nanotechnology Infrastructure Network.

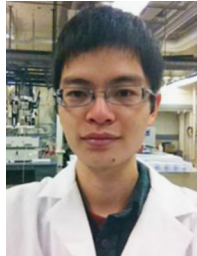
References

- [1] Z.L. Wang, J.H. Song, *Science* 312 (2006) 242-246.
- [2] Z.L. Wang, G. Zhu, Y. Yang, S.H. Wang, C.F. Pan, *Mater. Today* 15 (2012) 532-543.
- [3] X.D. Wang, J.H. Song, J. Liu, Z.L. Wang, *Science* 316 (2007) 102-105.
- [4] K.I. Park, S. Xu, Y. Liu, G.T. Hwang, S.J.L. Kang, Z.L. Wang, K.J. Lee, *Nano Lett.* 10 (2010) 4939-4943.
- [5] M. Yanchao, Z. Ping, G. McConohy, Y. Hao, T. Yexiang, W. Xudong, *Adv. Energy Mater.* 4 (2014) 1301624-1301627.
- [6] W. Zeng, X.-M. Tao, S. Chen, S. Shang, H.L.W. Chan, S.H. Choy, *Energy Environ. Sci.* 6 (2013) 2631-2638.
- [7] Z.L. Wang, *ACS Nano* 7 (2013) 9533-9557.
- [8] Y. Yang, W.X. Guo, K.C. Pradel, G. Zhu, Y.S. Zhou, Y. Zhang, Y.F. Hu, L. Lin, Z.L. Wang, *Nano Lett.* 12 (2012) 2833-2838.
- [9] Y. Yang, J.H. Jung, B.K. Yun, F. Zhang, K.C. Pradel, W.X. Guo, Z.L. Wang, *Adv. Mater.* 24 (2012) 5357-5362.
- [10] Y. Yang, Y.S. Zhou, J.M. Wu, Z.L. Wang, *ACS Nano* 6 (2012) 8456-8461.
- [11] Y. Yang, Z.H. Lin, T. Hou, F. Zhang, Z.L. Wang, *Nano Res.* 5 (2012) 888-895.
- [12] Y. Yang, K.C. Pradel, Q.S. Jing, J.M. Wu, F. Zhang, Y.S. Zhou, Y. Zhang, Z.L. Wang, *ACS Nano* 6 (2012) 6984-6989.
- [13] Z.L. Wang, *Adv. Mater.* 24 (2012) 280-285.
- [14] Z. Yayu, D. Ping, N. Yuxin, W. Pinglei, Z. Yan, X. Lili, X. Xinyu, *Biosens. Bioelectron.* 57 (2014) 269-275.
- [15] Z. Yayu, L. Xuan, D. Ping, N. Yuxin, Z. Yan, X. Lili, X. Xinyu, *Nanotechnology* 25 (2014) 115502-115506.
- [16] N. Yuxin, D. Ping, Z. Yayu, W. Pinglei, X. Lili, Z. Yan, X. Xinyu, *Nanotechnology* 25 (2014) 265501-265509.
- [17] H.L. Zhang, Y. Yang, Y.J. Su, J. Chen, C.G. Hu, Z.K. Wu, Y. Liu, C.P. Wong, Y. Bando, Z.L. Wang, *Nano Energy* 2 (2013) 693-701.
- [18] Z.H. Lin, G. Cheng, Y. Yang, Y.S. Zhou, S. Lee, Z.L. Wang, *Adv. Funct. Mater.* 24 (2014) 2810-2816.
- [19] S. Bai, Q. Xu, L. Gu, F. Ma, Y. Qin, Z.L. Wang, *Nano Energy* 1 (2012) 789-795.
- [20] T.T. Pham, K.Y. Lee, J.-H. Lee, K.-H. Kim, K.-S. Shin, M.K. Gupta, B. Kumar, S.-W. Kim, *Energy Environ. Sci.* 6 (2013) 841-846.
- [21] M. Lee, J. Bae, J. Lee, C.S. Lee, S. Hong, Z.L. Wang, *Energy Environ. Sci.* 4 (2011) 3359-3363.
- [22] J.W. Zhong, Y. Zhang, Q.Z. Zhong, Q.Y. Hu, B. Hu, Z.L. Wang, J. Zhou, *ACS Nano* 8 (2014) 6273-6280.
- [23] J.H. Lee, K.Y. Lee, M.K. Gupta, T.Y. Kim, D.Y. Lee, J. Oh, C. Ryu, W.J. Yoo, C.Y. Kang, S.J. Yoon, J.B. Yoo, S.W. Kim, *Adv. Mater.* 26 (2014) 765-769.
- [24] C. Xu, Z.L. Wang, *Adv. Mater.* 23 (2011) 873-877.
- [25] D.Y. Lee, H. Kim, H.M. Li, A.R. Jang, Y.D. Lim, S.N. Cha, Y.J. Park, D.J. Kang, W.J. Yoo, *Nanotechnology* 24 (2013). Q8
- [26] A. Kathalingam, S. Valanarasu, V. Senthilkumar, J.K. Rhee, *Mater. Chem. Phys.* 138 (2013) 262-269.
- [27] Y. Yang, H.L. Zhang, Y. Liu, Z.H. Lin, S. Lee, Z.Y. Lin, C.P. Wong, Z.L. Wang, *ACS Nano* 7 (2013) 2808-2813.
- [28] Z.L. Wang, *MRS Bull.* 32 (2007) 109-116.
- [29] Z.L. Wang, *Adv. Funct. Mater.* 18 (2008) 3553-3567.
- [30] Z.L. Wang, R.S. Yang, J. Zhou, Y. Qin, C. Xu, Y.F. Hu, S. Xu, *Mater. Sci. Eng. R* 70 (2010) 320-329.
- [31] Z.L. Wang, *MRS Bull.* 37 (2012) 814-827.
- [32] Z.L. Wang, *Mater. Sci. Eng. R* 64 (2009) 33-71.
- [33] Z.L. Wang, W.Z. Wu, *SPIE Newsroom* (2014).
- [34] X. Wang, *Nano Energy* 1 (2012) 13-24.
- [35] B. Kumar, S.-W. Kim, *Nano Energy* 1 (2012) 342-355.
- [36] B. Kumar, K. Sang-Woo, J. Mater. Chem. 21 (2011) 18946-18958.
- [37] Z.L. Wang, J. Song, *Science* 312 (2006) 242.
- [38] Y.-F. Lin, J. Song, Y. Ding, S.-Y. Lu, Z.L. Wang, *Appl. Phys. Lett.* 92 (2008) 022105.
- [39] M.-Y. Lu, J. Song, M.-P. Lu, C.-Y. Lee, L.-J. Chen, Z.L. Wang, *ACS Nano* 3 (2009) 357-362.
- [40] C.-T. Huang, J. Song, W.-F. Lee, Y. Ding, Z. Gao, Y. Hao, L.-J. Chen, Z.L. Wang, *J. Am. Chem. Soc.* 132 (2010) 4766-4771.
- [41] C. Chang, V.H. Tran, J. Wang, Y.-K. Fuh, L. Lin, *Nano Lett.* 10 (2010) 726-731.
- [42] X. Chen, S. Xu, N. Yao, Y. Shi, *Nano Lett.* 10 (2010) 2133-2137.
- [43] K.-I. Park, S. Xu, Y. Liu, G.-T. Hwang, S.-J.L. Kang, Z.L. Wang, K.J. Lee, *Nano Lett.* 10 (2010) 4939-4943.
- [44] J.H. Jung, M. Lee, J.-I. Hong, Y. Ding, C.-Y. Chen, L.-J. Chou, Z.L. Wang, *ACS Nano* 5 (2011) 10041-10046.
- [45] T.I. Lee, S. Lee, E. Lee, S. Sohn, Y. Lee, S. Lee, G. Moon, D. Kim, Y.S. Kim, J.M. Myoung, Z.L. Wang, *Adv. Mater.* 25 (2013) 2920-2925.
- [46] S. Hoffmann, F. Östlund, J. Michler, H.J. Fan, M. Zacharias, S.H. Christiansen, C. Ballif, *Nanotechnology* 18 (2007) 205503.
- [47] Z. Gao, Y. Ding, S. Lin, Y. Hao, Z.L. Wang, *Phys. Status Solidi RRL* 3 (2009) 260-262.
- [48] P. Li, Q. Liao, S. Yang, X. Bai, Y. Huang, X. Yan, Z. Zhang, S. Liu, P. Lin, Z. Kang, Y. Zhang, *Nano Lett.* 14 (2014) 480-485.
- [49] Y. Gao, Z.L. Wang, *Nano Lett.* 9 (2009) 1103-1110.
- [50] Handbook of optical constants of solids, Academic Press, 1998. Q9
- [51] A.J. Lovinger, D.D. Davis, R.E. Cais, J.M. Kometani, *Macromolecules* 19 (1986) 1491-1494.
- [52] T.R. Dargaville, M. Celina, P.M. Chaplya, J. Polym. Sci. Part B: Polym. Phys. 43 (2005) 1310-1320.

- [53] H.H. Law, P.L. Rossiter, G.P. Simon, J. Unsworth, *J. Mater. Sci.* 30 (1995) 4901-4905.
- [54] T. Shroud, S. Zhang, *J. Electroceram.* 19 (2007) 113-126.
- [55] J. Anderson, G.V.D.W. Chris, *Rep. Prog. Phys.* 72 (2009) 126501.
- [56] Y. Hu, B.D.B. Klein, Y. Su, S. Niu, Y. Liu, Z.L. Wang, *Nano Lett.* 13 (2013) 5026-5032.
- [57] Z. Zhang, K. Yao, Y. Liu, C. Jin, X. Liang, Q. Chen, L.M. Peng, *Adv. Funct. Mater.* 17 (2007) 2478-2489.
- [58] Y. Zhang, Y. Liu, Z.L. Wang, *Adv. Mater.* 23 (2011) 3004-3013.
- [59] G.A. Shi, M. Stavola, S.J. Pearton, M. Thieme, E.V. Lavrov, J. Weber, *Phys. Rev. B* 72 (2005) 195211.
- [60] F. Chaabouni, M. Abaab, B. Rezig, *Sens. Actuators B* 100 (2004) 200-204.
- [61] Z. Fan, D. Wang, P.-C. Chang, W.-Y. Tseng, J.G. Lu, *Appl. Phys. Lett.* 85 (2004) 5923-5925.
- [62] X. Xue, Y. Nie, B. He, L. Xing, Y. Zhang, Z.L. Wang, *Nanotechnology* 24 (2013) 225501.
- [63] Y. Hu, L. Lin, Y. Zhang, Z.L. Wang, *Adv. Mater.* 24 (2012) 110-114.
- [64] M. Hussain, M.A. Abbasi, Z.H. Ibupoto, O. Nur, M. Willander, *Phys. Status Solidi A - Appl. Mater. Sci.* 211 (2014) 455-459.
- [65] D. Zhu, Y. Fu, W. Zang, Y. Zhao, L. Xing, X. Xue, *Sens. Actuators B* 205 (2014) 12-19.
- [66] S.R. Morrison, *Sens. Actuators* 2 (1981) 329-341.
- [67] E. Traversa, *Sens. Actuators B* 23 (1995) 135-156.
- [68] A.C. Caballero, M. Villegas, J.F. Fernández, M. Viviani, M. T. Buscaglia, M. Leoni, *J. Mater. Sci. Lett.* 18 (1999) 1297-1299.
- [69] W. Jing, W. Hui, L. Qiuhsia, *Meas. Sci. Technol.* 14 (2003) 172.
- [70] Y. Isogai, M. Miyayama, H. Yanagida, *Ceram. Trans.* 43 (1993) 385-392.
- [71] W. Heywang, *J. Mater. Sci.* 6 (1971) 1214-1224.
- [72] M. Viviani, M.T. Buscaglia, V. Buscaglia, M. Leoni, P. Nanni, *J. Eur. Ceram. Soc.* 21 (2001) 1981-1984.
- [73] J. Nowotny, M. Rekas, *Ceram. Int.* 20 (1994) 265-275.
- [74] Y. Zhao, X. Lai, P. Deng, Y. Nie, Y. Zhang, L. Xing, X. Xue, *Nanotechnology* 25 (2014) 115502.
- [75] C. Pan, R. Yu, S. Niu, G. Zhu, Z.L. Wang, *ACS Nano* 7 (2013) 1803-1810.
- [76] Y. Zhao, P. Deng, Y. Nie, P. Wang, Y. Zhang, L. Xing, X. Xue, *Biosens. Bioelectron.* 57 (2014) 269-275.
- [77] S. Min Kim, H. Kim, Y. Nam, S. Kim, *Sens. Actuators B* 2 (2012) 042174.
- [78] K.Y. Lee, B. Kumar, J.-S. Seo, K.-H. Kim, J.I. Sohn, S.N. Cha, D. Choi, Z.L. Wang, S.-W. Kim, *Nano Lett.* 12 (2012) 1959-1964.
- [79] G.H. Jain, S. Nahire, D. Kajale, G. Patil, S. Shinde, D. Chavan, V. Gaikwad, Cr₂O₃-doped BaTiO₃ as an ammonia gas sensor, *New Developments and Applications in Sensing Technology*, Springer157-167.
- [80] S.C. Roy, G.L. Sharma, M.C. Bhatnagar, S.B. Samanta, *Sens. Actuators B* 110 (2005) 299-303.
- [81] J.S. Forsythe, D.J.T. Hill, *Prog. Polym. Sci.* 25 (2000) 101-136.
- [82] T.R. Dargaville, M. Celina, R.L. Clough, *Radiat. Phys. Chem.* 75 (2006) 432-442.
- [83] D. Parks, B. Tittmann, *IEEE Trans. Ultrason. Ferroelectr. Freq. Control* 61 (2014) 1216-1222.
- [84] S. Dhara, P.K. Giri, *Nanoscale Res. Lett.* 6 (2011) 1-8.
- [85] C. Soci, A. Zhang, B. Xiang, S.A. Dayeh, D.P.R. Aplin, J. Park, X.Y. Bao, Y.H. Lo, D. Wang, *Nano Lett.* 7 (2007) 1003-1009.
- [86] J. Liu, P. Fei, J. Song, X. Wang, C. Lao, R. Tummala, Z.L. Wang, *Nano Lett.* 8 (2008) 328-332.
- [87] Q.H. Li, T. Gao, Y.G. Wang, T.H. Wang, *Appl. Phys. Lett.* 86 (2005) 123117.
- [88] X.N. Wen, Y.J. Su, Y. Yang, H.L. Zhang, Z.L. Wang, *Nano Energy* 4 (2014) 150-156.
- [89] P. Ehrlich, *J. Res. Natl. Bur. Stand.* 51 (1953) 185-188.
- [90] B.B. Owen, R.C. Miller, C.E. Milner, H.L. Cogan, *J. Phys. Chem.* 65 (1961) 2065-2070.
- [91] Z.H. Lin, G. Cheng, L. Lin, S. Lee, Z.L. Wang, *Angew. Chem. Int. Ed.* 52 (2013) 12545-12549.
- [92] L.S. McCarty, G.M. Whitesides, *Angew. Chem. Int. Ed.* 47 (2008) 2188-2207.
- [93] Y. Su, X. Wen, G. Zhu, J. Yang, J. Chen, P. Bai, Z. Wu, Y. Jiang, Z.L. Wang, *Nano Energy* 9 (2014) 186-195. Q11
- [94] Z.-H. Lin, G. Zhu, Y.S. Zhou, Y. Yang, P. Bai, J. Chen, Z. L. Wang, *Angew. Chem. Int. Ed.* 52 (2013) 5065-5069.
- [95] M.D. Hogue, C.R. Buhler, C.I. Calle, T. Matsuyama, W. Luo, E. E. Groop, *J. Electrost.* 61 (2004) 259-268.
- [96] V. Nguyen, R. Yang, *Nano Energy* 2 (2013) 604-608.
- [97] W. Wu, L. Wang, Y. Li, F. Zhang, L. Lin, S. Niu, D. Chenet, X. Zhang, Y. Hao, T.F. Heinz, J. Hone, Z.L. Wang, *Nature* 514 (2014) 470-474.



Vu Nguyen received his B.S. degree in Mechanical Engineering from Worcester Polytechnic Institute, Worcester, Massachusetts in 2012. He is currently pursuing Ph.D. degree at the University of Minnesota, Minneapolis, Minnesota. His research interests are energy harvesting and self-powered systems at micro/nanoscale.



Ren Zhu received his B.S. degree in Mechanical Engineering and Automation from Shanghai Jiao Tong University, China, in 2010. He is currently a Ph.D. candidate at University of Minnesota. His research is mainly focused on mechanical energy harvesting and strain sensing based on piezoelectric nanostructures.



Rusen Yang received his Ph.D. degree in Materials Science and Engineering from Georgia Institute of Technology in 2007, where he continued as Post-Doctoral Associate. He joined Mechanical Engineering at the University of Minnesota-Twin Cities as an assistant professor in 2010. He has discovered novel nanostructures, such as ZnO, SnO₂, Zn₃P₂, and investigated their application potentials. His most recent work on energy harvester based on piezoelectric nanomaterials made significant contribution in the field of renewable energy.